International Journal of Polymer Analysis and Characterization

ISSN: (Print) (Online) Journal homepage: https://www.tandfonline.com/loi/gpac20

Influence of nanosized $CaCO_3$ content in tailoring the structure, the morphology and the thermal and mechanical properties of iPP/PA66/PP-g-MA alloy

Safieddine Bahlouli, Azzedine Makhlouf & Nacerddine Haddaoui

To cite this article: Safieddine Bahlouli, Azzedine Makhlouf & Nacerddine Haddaoui (2021): Influence of nanosized $CaCO_3$ content in tailoring the structure, the morphology and the thermal and mechanical properties of iPP/PA66/PP-g-MA alloy, International Journal of Polymer Analysis and Characterization, DOI: 10.1080/1023666X.2021.1902675

To link to this article: https://doi.org/10.1080/1023666X.2021.1902675

Published online: 29 Mar 2021.

INTERNATIONAL JOURNAL OF POLYMER ANALYSIS AND CHARACTERIZATION
https://doi.org/10.1080/1023666X.2021.1902675

Taylor & Francis
Taylor & Francis Group

Influence of nanosized $CaCO_3$ content in tailoring the structure, the morphology and the thermal and mechanical properties of iPP/PA66/PP-g-MA alloy

Safieddine Bahlouli[a,b], Azzedine Makhlouf[b,c], and Nacerddine Haddaoui[a]

[a]Laboratoire de Physico-Chimie des Hauts Polymères, UFAS1: Université Ferhat Abbas, Sétif, Algeria; [b]Département de Génie Industriel, Université Abbès Laghrour, Khenchela, Algeria; [c]Laboratoire des Silicates, Polymères et Nanocomposites, Guelma, Algeria

ABSTRACT

Nanocomposites of Polypropylene/Polyamide 66 (iPP/PA66) with a weight ratio of (70/30) filled with stearic acid-treated nanosized $CaCO_3$ were melt compounded in the presence of a fixed amount of grafted polypropylene maleic anhydride (PP-g-MA) in a Brabender mixer. The purpose of this research is to obtain nanocomposites with high-performance structural, morphological, and thermomechanical properties. The obtained properties are discussed in light of the content of nano-$CaCO_3$ and of the induced interfacial bonding properties generated by the insertion of the compatibilizer. The results confirmed that, according to the FTIR spectroscopy analysis, the existence, on one hand of possible interactions between PP-g-MA and PA66 and, on the other hand, between stearic acid and PA66. XRD results show that nanosized $CaCO_3$ particles play the role of nucleating agents in the matrix and thus increasing the crystallinity of the blend. SEM results revealed that the treated nanosized $CaCO_3$ was more homogeneously dispersed in the (iPP/PA66), and a refinement of the morphology and better dispersion of the filler were detected after the addition of PP-g-MA. From the mechanical point of view; the incorporation of $CaCO_3$ increased appreciably the tensile strength at break and the tensile modulus of (iPP/PA66) blend.

ARTICLE HISTORY
Received 17 July 2020
Accepted 9 March 2021

KEYWORDS
Polypropylene; polyamide 66; nanosized-$CaCO_3$; compatibilizer; nanocomposites

Introduction

Academic and industrial research has constantly focused on polymer blends to fulfill the increasingly demanding challenges of the polymer industry to produce novel tailor-made polymeric materials with enhanced specific properties that single basic polymers lack. It is a convenient attractive and effective method for designing new high-performance polymers.[1,2]

Polypropylene (PP), is a low-cost material that has excellent characteristics such as high strength, good dimensional stability, friction resistance, and chemical resistance.[2] Therefore, considerable research has been published on the development of blends where PP is the continuous dominant phase.[3] Modification of polypropylene (PP) by the preparation of polypropylene/polyamide 6 (PP/PA6) blends has numerous potential advantages. Their blends can be tailored to obtained new materials that synergistically combine the excellent thermomechanical properties and abrasion resistance of polyamide with the insensitivity to humid environments, excellent hinge properties, and easy processability of polypropylene. However, since its chain structure is

CONTACT Nacerddine Haddaoui n_haddaoui@yahoo.com Laboratoire de Physico-Chimie des Hauts Polymères, UFAS-1: Université Ferhat Abbas, route de Scipion, 19000 Sétif, Algeria.

non-polar, it is somewhat a difficult task to combine polypropylene with polar organic phases such as the polyamides. Therefore, both PP and PA are immiscible and incompatible in nature due to their different chemical polarities and also to their dissimilar crystalline structures inducing phase separation in the mixture leading generally to poor mechanical properties of the materials.[4] To overcome these problems related to phase separation in the obtained blend; extensive research[5–11] has been reported on the use of a compatibilizer to promote chemical and/or physical affinity. Most frequently, the compatibilizer is a block or graft copolymer chain composed of two different blocks where each block has a given chemical and physical affinity with the respective blend phases. Polypropylene grafted with maleic anhydride (PP-g-MA) is one of the most frequently utilized compatibilizers that promotes interfacial interactions between the two polymer phases and thus enhancing the end-use of obtained blend.[5] Jaziri et al.[6] reported that the dispersion of recycled PA6 in the PP continuous phase and the interfacial adhesion was also improved, as a result of the creation of interphase that was formed by the interaction between the formed PP-g-PA6 copolymer. This interphase induced an improvement in tensile, thermal, viscoelastic properties of the blends of recycled PA6. Sacchi et al.[7] reported that maleic anhydride grafted polypropylene is very effective to induce dispersion of recycled PA66 into PP thus promoting interfacial adhesion that led to an improvement of the flexural strength. Ide et al.[8] described also the influence of PP-g-MA on (PP/PA6) polymer blends. The structural stability and morphology of the blends were effectively improved by (PP/PA6) grafted copolymers that were formed by the in situ reaction of anhydride groups with the amino end groups of PA6. Cheng et al.[9] reported that the effect of maleic anhydride grafted polypropylene, in the presence of organoclay, on the morphology of polypropylene (PP/PA66) blend was remarkable. They observed a transition from typical sea-island morphology to coarse co-continuous morphology and then to rod-like morphology with increasing compatibilizer contents. Particle filters have been extensively used in producing polymer composites with enhanced modulus, strength, rigidity, durability, and hardness. However, these properties enhancements are usually accompanied by a severe decrease in impact strength. Because of its abundance on earth, calcium carbonate ($CaCO_3$) is one of the least expensive compounding materials used in the plastics industry. Originally, the main purpose of adding micrometric-sized calcium carbonate particles as fillers for plastics was to reduce material costs. Aljoumaa et al.[10] observed that the size of the $CaCO_3$ particles, the shape, the surface treatment, and the fraction by weight of the filler have a noticeable marked effect on the mechanical properties of the PVC composite.[10,11] It has also been reported that the addition of microscale $CaCO_3$ particles to PP improves the mechanical and thermal behavior of the polymer.[3] Also, the insertion of $CaCO_3$ particles increased the modulus and tensile strength of neat PA66 however the elongation at yield and break is decreased. The introduction of nanoscale particles into a polymer matrix offers several direct advantages compared to conventional micron fillers. Nanosized $CaCO_3$ was superior to microsized $CaCO_3$, in that, it caused higher modulus and strength.[11]

However, and most frequently, it is necessary to increase the interactions between the filler and the matrix. More recently, the incorporation of precipitated calcium carbonate (PCC) particles with fine and ultrafine particles down to 40 nm in polymers are taking an important place in the polymer industry because of its larger contact surface compared to particles micrometric for the same load ratio.[12] The properties of polymers may therefore be modified by incorporating inorganic nanoparticles into the polymer matrix and the resulting properties of the obtained nanocomposites are often amplified several orders of magnitude higher than those of micro composites. The ultimate properties of nanocomposites depend on several parameters, including the nature, shape, size, and ratio of the particles inserted as well as the interface between the polymer and the nanoparticles.[11,13–15] The dispersion and the interfacial interactions between the nanofillers and the polymer matrix are essential to obtain improved properties of these nanocomposites.[16] Furthermore, $CaCO_3$ particles are often coated with stearic acid to control moisture

absorption, improve dispersion, and promote better polymer-particle contact. The effect of stearic acid as an interface modifier of calcium carbonate has been extensively reported.[17–19] Chan et al.[20] reported that the large specific surface of the nano-reinforcements leads to the formation of significant volume interphase leading to a good fillers dispersion resulting in a significant enhancement in the elastic modulus of (PP/nano-$CaCO_3$) composites.

The purpose of this research is to obtain nanocomposites with high-performance structural, morphological, and thermomechanical properties by improving the compatibility of polyamide 66 and polypropylene and enhancing the fixation of nanometric $CaCO_3$ particles onto the obtained blend. Furthermore; the effects of the content of nanosized $CaCO_3$ particles with and without compatibilizer (PP-g-MA) on the morphological, structural, mechanical, and thermal properties of the prepared nanocomposites were investigated.

Materials and methods

Materials

Polypropylene (PP) (PP012) supplied by Sabic Co. (KSA) is an isotactic homopolymer with a melt flow index (MFI) of about 18.5 g/10 min (190 °C, 2.16). The polyamide 66 (PA66) (PA66-024) was supplied by Xiamen Keyuan Co. (China). The polymer shows a melt flow rate (MFR) of about 25 g/10 min (230 °C, 2.16 kg) PA66 was dried at 90 °C overnight prior to use. Nanosized particles of calcium carbonate (nano-$CaCO_3$) (NCC-602) purchased from Xiamen Haitaida Co. (China) have an average diameter of 50 nm and a specific surface of about 175 m^2/gr. Dicummyl peroxide (DCP, 98%) produced by Elf Atochem (Germany) was used as a radical initiator with a half-life ($t_{1/2}$) of about 1 min at 178 °C. Maleic anhydride (MA, 99%) with a molecular weight of 98.06 g/mol purchased from Aldrich was used as a grafting monomer. Stearic acid (SA) used as a coupling agent with a decomposition temperature of about 300 °C and a melting point of 69.5 °C was supplied by Henry-Franc Co. (France). All reagents were used as received without further purification.

Grafting process of polypropylene

Dicummyl peroxide DCP (0.1 wt.%) and maleic anhydride MA (2 wt.%) are dispersed and homogenized in excess of acetone. The obtained solution is used for the impregnation of the PP granules. The acetone is then evaporated at 60 °C in a vacuum oven for 12 h. The grafting process is carried out in the molten state in a single screw extruder. The obtained extrudates were subjected to grinding and then stored for further use in hermetic plastic bags to protect them from moisture.

Treatment of calcium carbonate by stearic acid

In order to reduce the inter-particle interactions and to promote the $CaCO_3$ particles with (PP/PA66) compatibility; stearic acid (SA) was used for surface treatment of the calcite nanometric filler. The surface-treatment of synthesized calcium carbonate nanoparticles was carried out as follows: 1 g of stearic acid and 99 g of nanometric $CaCO_3$ previously dried under vacuum at 100 degrees overnight were dissolved in toluene and mechanically stirred at 50 rpm for 12 h. The mixture was then filtered and rinsed four times. The filler was then dried at 60 °C under a low vacuum for 24 h and stored for further use. The treatment of calcium carbonate by stearic acid has been previously reported by several authors.[17–19]

Elaboration of nanocomposites (sample preparation)

The different nanocomposite formulations were performed by dispersing of nanometric $CaCO_3$ in (PP/PA66) and (PP/PA66/PP-g-MA) in Brabender Plastograph BL2100 mixer (Germany) at 265 °C, using a rotor speed of 60 rpm for around 10 min. The resulting (PP/PA66/$CaCO_3$) nanocomposites is hence composed of (1, 3, 5, and 7 wt.%) of nano-$CaCO_3$ and 10 wt.% of compatibilizer PP-g-MA[21]. After pelletizing, the composite granules were compression molded using a hydraulic press Zwick 7102 at 200 °C and under a pressure of 200 Kg/cm^2 for 6 min. Prior to the elaboration of the composites; PP and PA66 were mixed together in the plastograph Brabender for 10 min at 265 °C.

Experimental

Infrared spectroscopic analysis (FTIR)

Spectra of films of the different blend formulations were recorded at room temperature on a Perkin Elmer Spectrum RX1). A spectrometer in a transmission mode at 4 cm^{-1} with the coaddition of 32 scans and a spectral range of 500–4000 cm^{-1}.

Wide-angle X-ray scattering (WAXS)

The apparatus used is of type Bruker D8 ECO. This apparatus is equipped with a copper anticathode tube emitting a light wave of length $K\alpha_1 =$ 0.15406 nm. The excitation conditions are: U = 40 kV of tension, I = 20 mA of current, 2°/min and the angle 2θ goes from 5° to 60°. All RX diffractograms have been processed by using EVA software.

Scanning electron microscopy (SEM)

The observations have been made on a Quanta 200 device in topographic mode on surfaces of samples made conductive by metallization (Au deposit). The samples were previously cryogenically fractured after being immersed in liquid nitrogen for about 5 min to have brittle fracture facies. The electron acceleration voltage retained is 20 kV so as to avoid any risk of degradation of the samples.

Thermogravimetric analysis (TGA)

Thermogravimetric analysis (TGA) has been performed using NETZSCH STA 449 F3 Jupiter equipment. All tests are conducted on samples with an average mass of 20 mg, the study was in the temperature range of 20–800 °C and at the heating rate of 10 °C/min and under nitrogen flow.

Mechanical behavior

Tensile tests

Specimens according to ASTM-D 638 of all (PP/PA66/nanosized $CaCO_3$) composites were subjected to tensile tests using an Instron mechanical tester (MTC 5569) with a crosshead speed of 30 mm/min. The reported measured properties (Young's modulus, stress, and deformation at break) are average values from five different specimens.

Impact test

The Izod impact strengths of different (PP/PA66) blends were determined using a Pendulum Impact Testing Machine: Impactor CEAST 9050 with an impact energy of 7.5 KJ according to

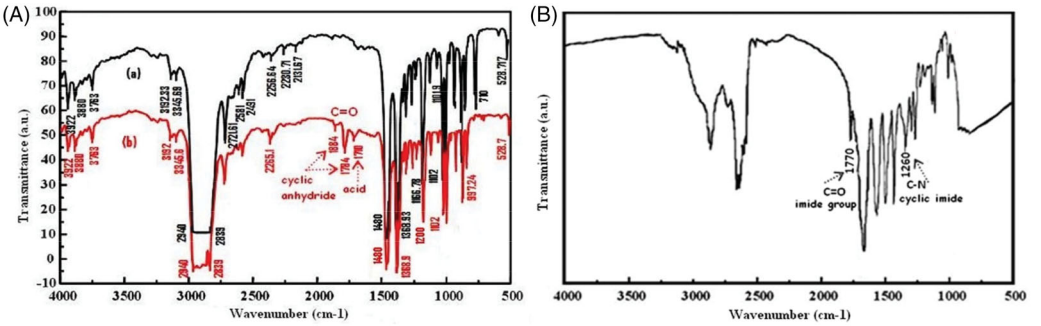

Figure 1. (A) FTIR spectrum of: (a) polypropylene and (b) polypropylene grafted with maleic anhydride PP-g-MA, (B) FTIR spectrum of PP/PA66 with PP-g-MA.

ASTM D 256-88. 1 mm V notched specimens were cut into a standard dimension of ($64 \times 12 \times 3.2$ mm). The measured values are of significance for a relative comparison between the neat and the different blended (PP/PA66) materials only. Five analyses were performed for each sample, and the average values are reported.

Results and discussion

FTIR

Figure 1 shows the infrared spectra of (PP-g-MA) in comparison with that of the neat PP (Figure 1Aa). The latter is distinguished by two well-documented characteristic absorption bands.[22] The peak at 2940 cm^{-1} corresponds to the asymmetric and symmetric stretching of the methyl group and the peak observed at 2839 cm^{-1} is attributed to the asymmetric and symmetric stretching of the methylene groups. However, three absorption peaks around 1884, 1784, and 1710 cm^{-1} can be distinguished on the spectrum of polypropylene grafted with maleic anhydride (Figure 1Ab) while the reference spectrum (Figure 1Aa) of neat polypropylene does not show any absorption bands in these regions. These peaks are then the proper characteristics of PP-g-MA.

Figure 1B shows a typical infrared spectrum of the (PP/PA66) (70/30) blend after the incorporation of PP-g-MA. The spectrum of the compatibilized blend displays two other peaks at 1770 and 1260 cm^{-1} were assigned to the carbonyl CO vibration and CN vibration of the imide group respectively due to the formation of imide linkage (Schema 1) compared to the infrared spectrum of the (PP/PA66) without compatibilizer (Figure 2A).

Figure 2B shows infrared spectra of (PP/PA66) with nanosized $CaCO_3$ treated by stearic acid showing absorptions for all required chemical groups: NH stretch at 3300 cm^{-1}, CH stretch at 2860–2980 cm^{-1}, Amide I at 1650 cm^{-1}, and Amide II at 1520 cm^{-1}. The band at NH stretching and CO stretching strongly depend on hydrogen bonding interaction between the PA66 chains, these results are supported by the reported literature.[23,24] $CaCO_3$ forms a complex with CH groups in polyamides and breaks the hydrogen bonds between PA66 chains. The appearance of a new band at 1020 cm^{-1} is characteristic of the valence vibration of the CN bond resulting from the reaction between PA66 and stearic acid (Schema 2). The other peaks correspond to PP at 2900, 1480, 1200, and 710 cm^{-1}. The esterification reaction promotes the compatibility between the molecular chains, thereby improving interfacial bonding in the (PP/PA66/PP-g-MA/$CaCO_3$) composites structural changes observed in the FTIR spectra after the addition of filler in PA66.[25] There were some significant changes observed in the IR absorption of the CH region. Changes in the peaks proved that the addition of filler in the matrix affects the absorbance of the polymer. It means that the interfacial effect would be a dominant factor where there is a direct

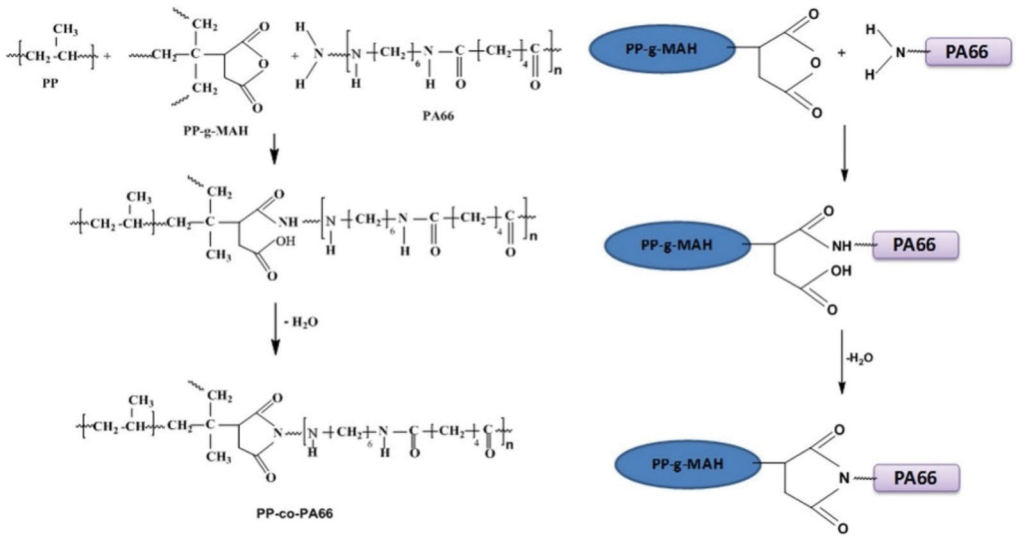

Schema 1. Schematic most probable reaction between PP-g-MA and PA66.

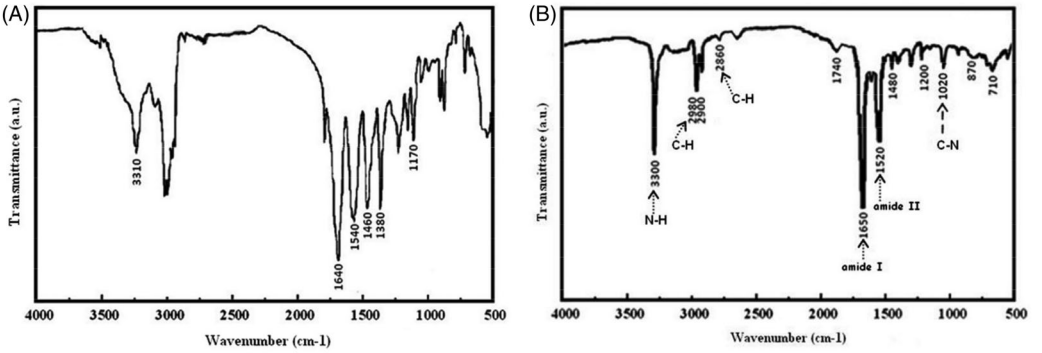

Figure 2. FTIR spectrum of (A) PP/PA66 without PP-g-MA, (B) PP/PA66 with treated nano-$CaCO_3$.

binding of the polymer and the filler. The FTIR spectra provided a possible mechanism between nanosized $CaCO_3$ treated by stearic acid and PA66 is illustrated below:

These results are in good agreement with the reported results by Basilia et al.[26] and by Seul et al.[27]. They reported that PA66 has an absorbance peak at 870 cm^{-1} which is due to the absorbance of the CO_3 group indicating the presence of $CaCO_3$.

Microstructural characterization

Figure 3A shows a typical powder (XRD) patterns of nanoparticles of $CaCO_3$, with peaks appeared at: $2\theta = 23°$, 29°, 36°, 39.5°, 43°, 47°, 47.5°, 57°, and 57.5°, with (012), (104), (110), (113), (202), (018), (116), (211) and (122) planes. The XRD patterns of (PP/PA66) and (PP/PA66/$CaCO_3$) composites are shown in Figure 3B.

The crystal structure of thermoplastics has been shown to have a significant effect on thermal and mechanical properties. An increase in crystallinity levels is recorded with the increase in the proportion of $CaCO_3$ introduced in the mixture. This result is due to $CaCO_3$ nanoparticles orienting the chain, and thus increasing the crystallinity. It is estimated that one of the important

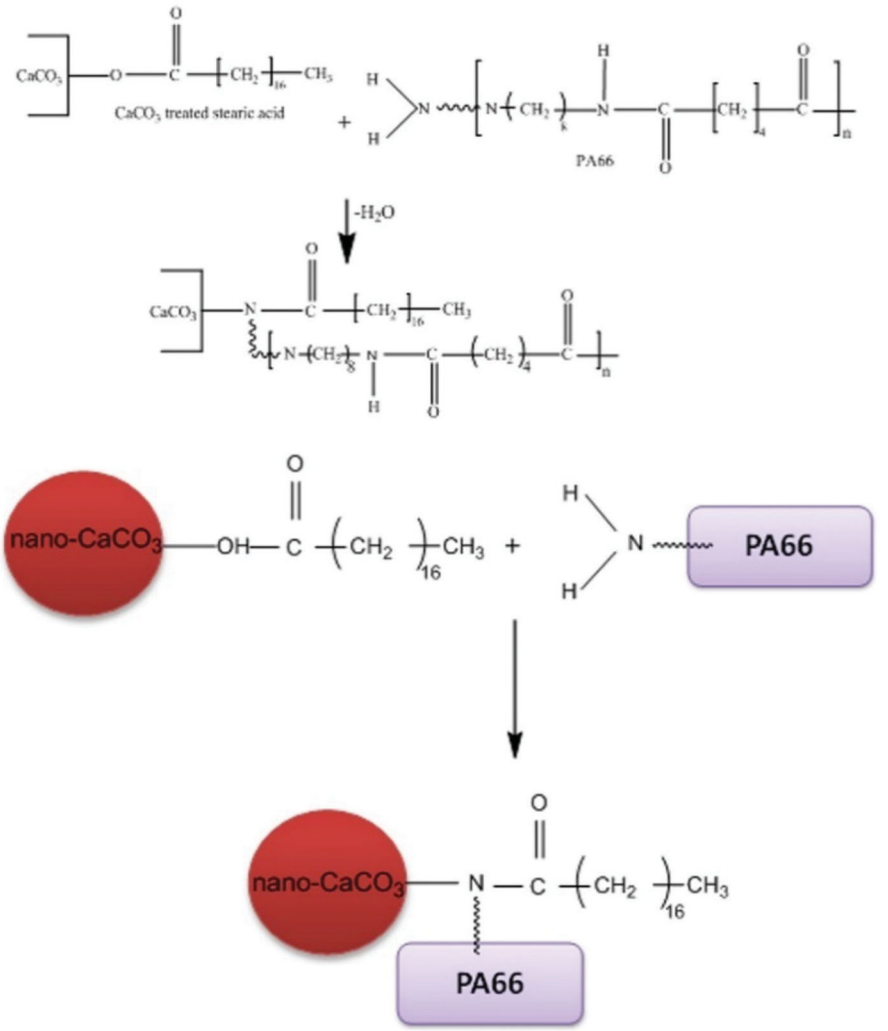

Schema 2. Schematic most probable reaction between PA66 and stearic acid.

factors of the increase in crystallinity is the formation of germs responsible for the crystallization of polymers, that is, their presence in the polymer and their good dispersion contribute to the increase in the number of crystallite seeds formed.[28] The increase in the crystallinity content with the increase in the filler ratio has been attributed to the nucleating effect of $CaCO_3$, in particular, the fillers which create several filler-filler and filler-matrix interactions especially between the stearic acid carried on the nano-$CaCO_3$ and the PA66. The smaller size of crystallites, the wider are the peaks. This effect becomes more pronounced for crystallites less than 1 μm in diameter.[23] This can be explained as follows: when crystallite is in Bragg condition for a plane (hkl) (i.e., $2\theta = 2\theta_{hkl}$), the rays diffracted by two successive atomic planes are in phase, so the intensities add up. Therefore, compared to a peak measured on a sample with large crystallites, there is an enlargement of the peak which is given by the formula of Scherrer (1918):[29]

$$D = \frac{k.\lambda}{\beta\cos(\theta)} \tag{1}$$

Where: D = crystallite size (nm), $k = 0.9$ (Scherrer constant), λ = wave length (0.1541 nm for $K\alpha$ line of copper), β = FWHM (radians), θ = peak position (radians).

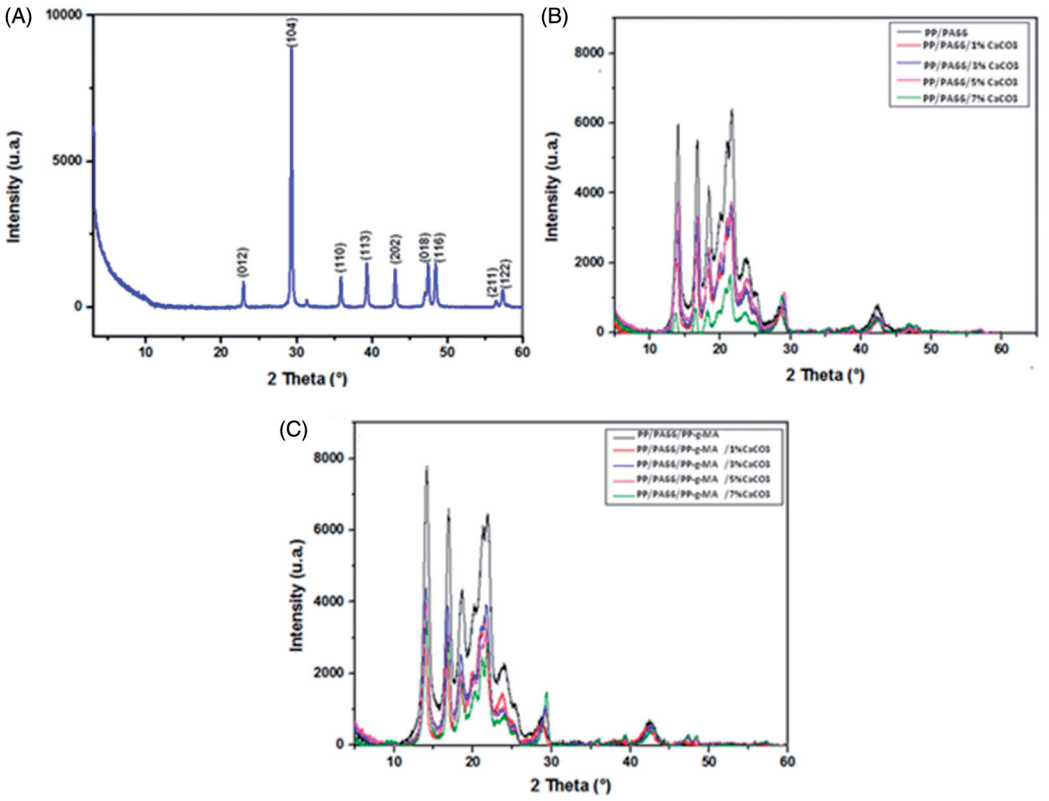

Figure 3. XRD curve of (A) treated nano-$CaCO_3$, (B) neat PP/PA66 and with 1, 3, 5, and 7% by weight of treated nano-$CaCO_3$, (C) neat PP/PA66/PP-g-MA and with 1, 3, 5, and 7% by weight of treated nano-$CaCO_3$.

Chatterjee et al.[30] in their study on the effect of micro and nano-$CaCO_3$/PMMA, mentioned that the interactions between the filler and the matrix are better in the case of nano-$CaCO_3$ than micro-$CaCO_3$ filler. This is mainly due to the fact that nanofillers have an important specific surface allowing more interactions with PMMA. They also observed that the smaller $CaCO_3$ size, the smaller spherulites formed and the crystallization rate will be faster. Khan et al.[31] focused on the effect of micro and nano-$CaCO_3$ size on the behavior of natural rubbers. They showed that the crystallinity ratio is higher in the case of nano-$CaCO_3$ than that with micro-$CaCO_3$ ones and the addition of treated nano-$CaCO_3$ fillers with stearic acid increases the crystallinity ratio. This important phenomenon in crystallinity is attributed to the process of germination and to the faster growth of the crystallites in the presence of calcium carbonate fillers.[32] Figure 3C shows the effect of incorporation of the PP-g-MA into the (PP/PA66) matrix leads to an increase in the degree of crystallinity with training (formation) of a PP-co-PA66 copolymer at the interface improving the compatibility between the two materials which were initially incompatible (Schema 1). Similar results are mentioned in the works of Ulrich et al.[33] on (PA66/PP) in presence of PP-g-MA. The results of crystallite size and the crystallinity ratio are shown in Table 1.

Morphology

Figure 4 shows the fracture surface of all studied composites. It is observed that the minority phase (PA66) is dispersed in the form of nodules in the PP matrix. There are no interactions between the two polymers initially incompatible (Figure 4A).

Table 1. Crystallites size and crystallinity ratio of (PP/PA66) with 5 wt. % $CaCO_3$ untreated and treated and (PP/PA66/PP-g-MA) with 5 wt. % $CaCO_3$ untreated and treated.

Material	Crystallite size (nm)	Crystallinity ratio Xc (%)
Neat PP	0.360	57.10
Neat PA 66	0.363	35.10
PP/PA 66	6.415	18.90
PP/PA 66/1% $CaCO_3$ Utr	0.314	48.94
PP/PA 66/3% $CaCO_3$ Utr	0.336	54.12
PP/PA 66/5% $CaCO_3$ Utr	5.006	70.22
PP/PA 66/7% $CaCO_3$ Utr	6.461	69.77
PP/PA 66 /1% $CaCO_3$ Tr	0.541	60.70
PP/PA 66 /3% $CaCO_3$ Tr	0.447	57.35
PP/PA 66/5% $CaCO_3$ Tr	2.448	46.90
PP/PA 66/7% $CaCO_3$ Tr	0.442	79.54
PP/PA 66/PP-g-MA	5.110	43.73
PP/PA 66/PP-g-MA/1% $CaCO_3$ Utr	0.319	52.71
PP/PA 66/PP-g-MA/3% $CaCO_3$ Utr	0.367	61.31
PP/PA 66/PP-g-MA/5% $CaCO_3$ Utr	0.376	60.10
PP/PA 66/PP-g-MA/7% $CaCO_3$ Utr	0.391	64.61
PP/PA 66/PP-g-MA/1% $CaCO_3$ Tr	0.407	54.27
PP/PA 66/PP-g-MA/3% $CaCO_3$ Tr	0.406	52.72
PP/PA 66/PP-g-MA/5% $CaCO_3$ Tr	0.336	49.39
PP/PA 66/PP-g-MA/7% $CaCO_3$ Tr	0.312	60.74

$CaCO_3$ Utr = $CaCO_3$ Untreated; $CaCO_3$ Tr = $CaCO_3$ Treated.

Figure 4B shows the SEM micrographs of (PP/PA66/PP-g-MA), a refinement of the morphology was observed after the addition of the PP-g-MA, the dispersion will be fine. PP-g-MA ensures continuity between PP and PA66 by the formation of the copolymer

PP-co-PA66 at the interface by the reaction of maleic anhydride with the amino groups at the end of PA66 during mixing (Schema 1). The domains are irregular and smaller than in the mixture without PP-g-MA inducing a ductile fracture facies with better dispersion of the different constituents of the mixture which improves impact resistance. Numerous studies[34,35] have also reported an improvement in morphologies of polyamide 6 and polypropylene compatibilized with anhydride-grafted polypropylene. Zeng et al.[36] noted a very strong interfacial adhesion between the PP and PA66 when adding the PP-g-MA. This considerably improves the compatibility of PP and PA66. Recently, Roeder et al.[37] have also studied the influence of PP-g-MA and showed that this improvement in interfacial adhesion resulted from the creation of the covalent bonds between the anhydride group of PP-g-MA and the (PP/PA6). Zoukrami et al.[38] reported the effect of compatibilizer PP-g-MA on (PP/SiO_2) behavior where a considerable improvement of the morphology is observed by a finer dispersion. Figures 4C and D represent respectively the morphologies of the (PP/PA66) mixtures in the presence of 5 wt.% of untreated and stearic acid (SA) treated nanosized particles of $CaCO_3$ with an average primary particle size of 50 nm. Numerous aggregates can be observed with the untreated samples where the nanoparticles have a strong tendency to form agglomerates because of the intrinsic high surface energy of the filler.[39] However, in the case of SA coated nano-$CaCO_3$; the treated particles become spherical and a better distribution of the particles in the (PP/PA66) matrix is observed (Figure 4D). Zhang et al.[40] their study of (PP/EOC) (copolymer-Ethylen-Octen) mixture reported that the adhesion between the matrix and the particles is superior for $CaCO_3$ with stearic acid shell compared to untreated nano-$CaCO_3$. Bonse et al.[41] studied the effect of micro and nano-$CaCO_3$ on the morphological behavior of the (PA6/$CaCO_3$) composite. SEM micrographs of nanocomposites revealed regular spherical shape while micrographs of composites with micro-$CaCO_3$ show agglomerates of needle and flake form and other forms under certain conditions. The SEM photomicrographs of compatibilized nanocomposites are illustrated in Figures 4E and F. Agglomeration of particles can be observed when the untreated nanofiller is incorporated in the compatibilized mixture.

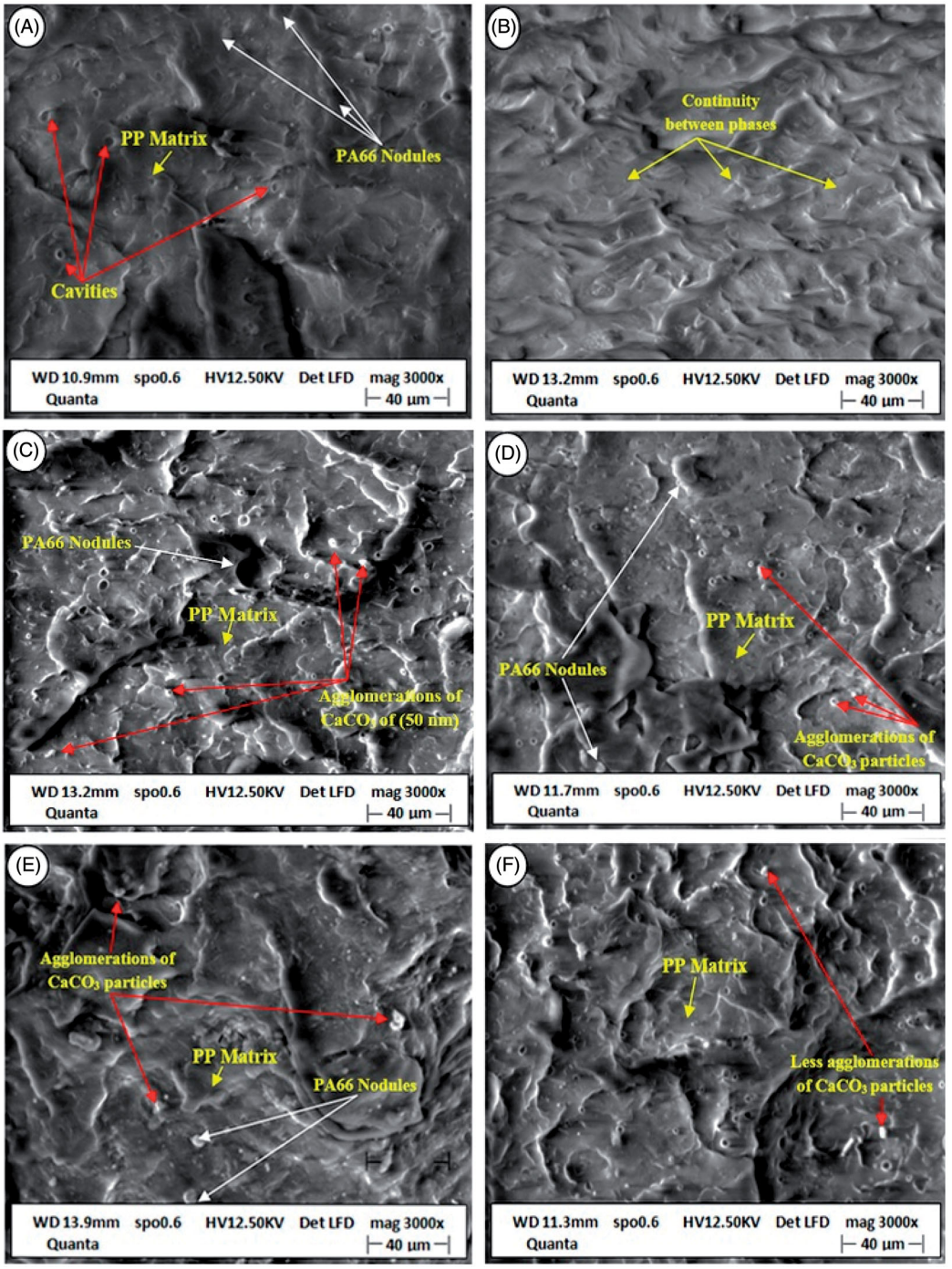

Figure 4. Scanning electron micrograph of (A) PP/PA66, (B) PP/PA66/PP-g-MA, (C) PP/PA66 with 5 wt.% of untreated nano-$CaCO_3$, (D) PP/PA66 with 5 wt.% of treated nano-$CaCO_3$, (E) PP/PA66/PP-g-MA with 5 wt.% of untreated nano-$CaCO_3$ and (F) PP/PA66/PP-g-MA with 5 wt.% of treated nano-$CaCO_3$.

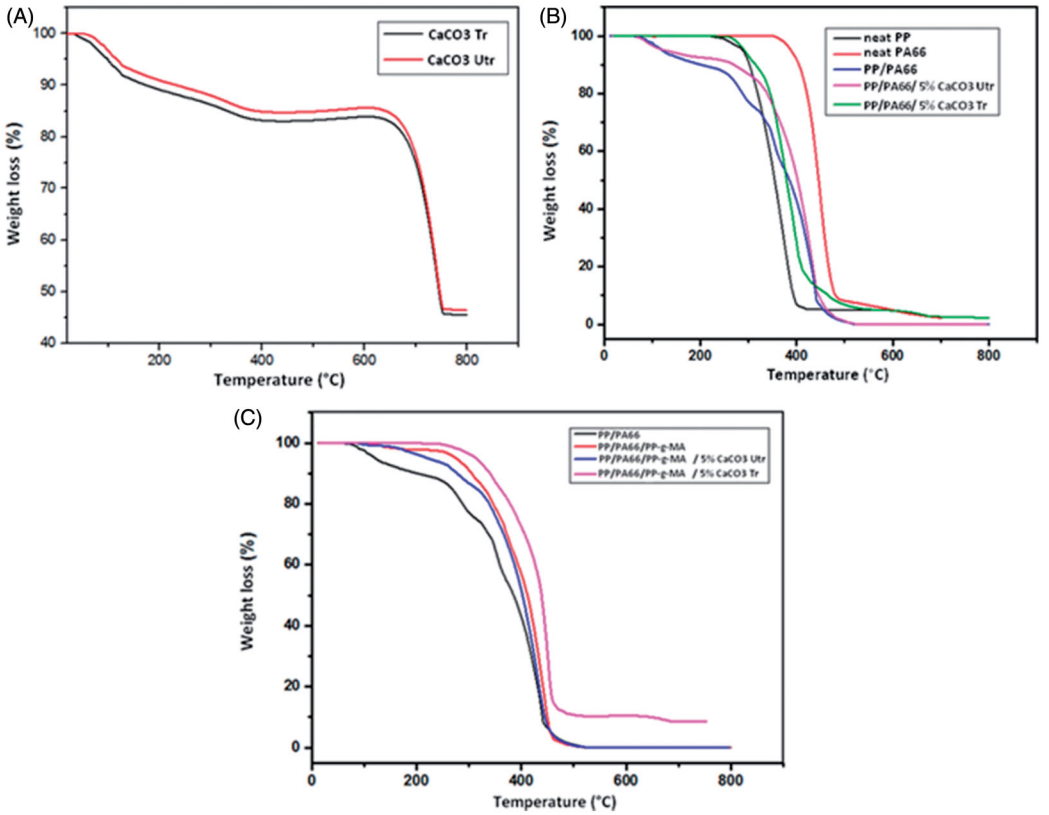

Figure 5. (A) Comparison of thermogravimetric analysis curves of untreated and treated nano-$CaCO_3$, (B) TGA curves of PP/PA66 with 5 wt.% of untreated and treated nano-$CaCO_3$ and (C) TGA curves of PP/PA66/PP-g-MA with 5 wt.% of untreated and treated nano-$CaCO_3$.

This phenomenon is visibly reduced (better dispersion) when both SA-treated fillers and the compatibilizer were incorporated. The reduction of the surface of the attraction forces between the nanoparticles forms a ductile facies which considerably improves impact resistance. According to the literature,[42] it has been found that there is a difference in morphology following the effect of micro and nano-$CaCO_3$ size.

Thermogravimetric analysis (TGA)

Thermogravimetric analysis (TGA) was conducted to monitor the degradation temperature and the thermal stability of the treated and untreated fillers of the studied composites with respect to filler treatment. The investigated formulations of (PP/PA66) alloys and their nanocomposites are shown in Figure 5 with Table 2 summarizes the respective onset and offset degradation temperatures derived from the thermogravimetric curves of all compounds. Thermograms of untreated nano-$CaCO_3$ and treated nano-$CaCO_3$ with stearic acid (SA) are shown in Figure 5A. A slight increase in the thermal stability of treated nano-$CaCO_3$ is observed. Moreover, the treated nano-$CaCO_3$ shows two weight loss stages of degradation reactions. The first step is a dehydration reaction that is mainly due to the evaporation of bonding water at 100 °C, and the release of the physisorbed water molecules. The second loss step occurs between 200 °C and 350 °C and is attributed to the decomposition of organic material (stearic acid) on the surface of the particles. No noticeable difference in the onset decomposition temperatures was observed with the (SA) treatment of the $CaCO_3$ (see Table 2).

Table 2. Data obtained through TGA of the PP/PA66 formulations with untreated and treated nano-$CaCO_3$.

Samples	T_{Onset}	T_{Offset}
$CaCO_3$ Utr	621.84	758.64
$CaCO_3$ Tr	620.12	757.41
Neat PP	225.11	427.52
Neat PA66	354.51	494.96
PP/PA66	230.15	501.80
PP/PA66/5% $CaCO_3$ Utr	254.87	520.61
PP/PA66/5% $CaCO_3$ Tr	258.08	531.55
PP/PA66/PP-g-MA	246.33	512.63
PP/PA66/PP-g-MA/5%$CaCO_3$ Utr	247.23	516.21
PP/PA66/PP-g-MA/5%$CaCO_3$ Tr	248.33	520.86

$CaCO_3$ Utr = $CaCO_3$ Untreated; $CaCO_3$ Tr = $CaCO_3$ Treated.

Figure 5B illustrates weight losses of neat PP, neat PA66, (PP/PA66) blend, and (PP/PA66) with treated and untreated $CaCO_3$ without compatibilizer PP-g-MA. From the thermograms profile, all samples presented the same trend with temperature and thermal stability. However, it can be seen that the addition of 5 wt.% of nanofillers ($CaCO_3$) induces a significant variation in terms of decomposition behavior as compared with the (PP/PA66) neat matrix. Other researchers[32,43] reported similar results where the optimum properties were found to be around 6 wt.% $CaCO_3$ content. This result is well illustrated with two temperatures characterizing these thermograms: T_{onset} and T_{offset}. For (PP/PA66) with 5 wt.% of treated $CaCO_3$ sample, the T_{onset} (258.08 °C) and T_{offset} (531.55 °C) shifted toward higher temperatures, indicating that the addition of nano-$CaCO_3$ treated can improve the thermal stability significantly. This result shows that the new composite (with 5 wt.% of treated $CaCO_3$) offers thermal stability of the order of 28 and 30 °C, respectively for the beginning and the end of the degradation compared to that of the neat matrix.

The process of the decomposition in (PP/PA66) with 5 wt.% untreated nano-$CaCO_3$ samples exhibited similar behavior with an increase of 24 °C and 19 °C in T_{onset} and T_{offset} respectively, compared to the neat matrix. The improved thermal stability is due to the barrier effect of nano-$CaCO_3$ particles against volatile gases formed during thermal degradation by creating a labyrinth or a "tortuous path" slowing the progression of gas molecules through the polymer matrix.[44] Tang et al.[45] reported also that the addition of micro-$CaCO_3$ or nano-$CaCO_3$, both treated by a titanium-based coupling agent, retarded the onset of degradation of polypropylene PP regardless of the particle size. Lam et al.[46] confirmed the improvement of the thermal stability of PP in presence of $CaCO_3$. The authors have highlighted the influence of surface treatment of treated $CaCO_3$ with sodium stearate. This effect is amplified in the presence of the compatibilizer in the neat matrix. This result indicates that the addition of PP-g-MA significantly improved the thermal stability of (PP/PA66) matrix. This could be attributed to the interaction between the maleic anhydride group of PP-g-MA and the amine group of PA66 leading to the formation of a PP-co-PA66 copolymer, acting as a compatibilizer. The introduction of nanofillers within the compatibilized mixture (PP/PA66/PP-g-MA) improves the thermal stability of the nanocomposites, especially with the treated nano-$CaCO_3$ (Figure 5C).

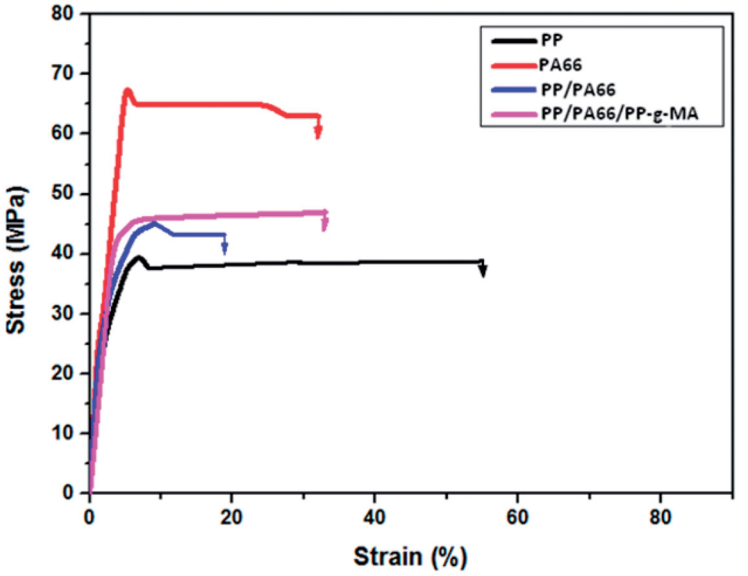

Figure 6. Typical stress–strain curves of PP, PA66, PP/PA66, and PP/PA66/PP-g-MA.

Kouini et al.[47] also showed that the addition of the compatibilizer PP-g-MA improves the thermal stability of the (PP/PA6/clay) system. Another study by Schlikmann et al.[39] on the micro and nano-$CaCO_3$ effect in PVC, showed that the composites formulated from nanofillers are more stable than those formulated with microfillers for the same load ratio of the filler. The work of Sadeghi et al.[42] on micro and nano (SBR/$CaCO_3$) system was able to show an improvement in thermal stability in the case of reinforcement by nanofillers by the formation of a layer on the surface that absorbs the heat of combustion. Bordes et al.[48] observed an increase in the onset decomposition temperature of 17 °C for (PP/$CaCO_3$) composites treated by stearic acid. This reduction in the particle size generally improves also the flame retardancy; this might be due to the nanofillers forming an effective layer on the surface, which absorbs the heat of burning. In conclusion, in the majority of cases, an improvement of the thermal stability of the polymers is observed with the addition of calcium carbonate.

Mechanical behavior

Tensile tests

Figure 6 shows the typical aspect of uniaxial tensile "stress–strain" curves for neat PP, neat PA66, and also for their blends (PP/PA66) with and without PP-g-MA. For all the formulations investigated, samples were tested at room temperature at crosshead speed set at 30 mm/min. As expected the PP exhibits a ductile thermoplastic behavior characterized by yield stress of around 40 MPa then a stable bearing tray characteristic of a plastic deformation until rupture at a stress of 39 MPa and an elongation at break of about 55%. The neat PA66 shows a strong and stiffly hard behavior with stress and strain values at break respectively of 70 MPa and 31%. Because of the incompatible nature of the (PP/PA66) matrix, a somewhat rigid behavior is observed with the blend and the elongation at break becomes less than that of the respective neat polymers. The fracture stress and the elongation at break are equal to 45 MPa and 9% respectively. However, the compatibilized composite exhibits a more ductile behavior. These results are comforted by other researchers.[49] The detailed tensile strength results of the different materials are presented in Table 3.

Table 3. Tensile properties of neat PP, neat PA66, neat and compatibilized (PP/PA66).

	Materials			
Properties	PP	PA66	PP/PA66	PP/PA66/PP-g-MA
Tensile strength, σ_b (MPa)	37 ± 0.1	62 ± 0.3	42 ± 0.3	46 ± 0.5
Modulus, E (MPa)	1500 ± 25	3200 ± 25	1720 ± 20	2030 ± 22
Elongation at break, ε_b (%)	55 ± 5	31 ± 10	19 ± 8	32 ± 10

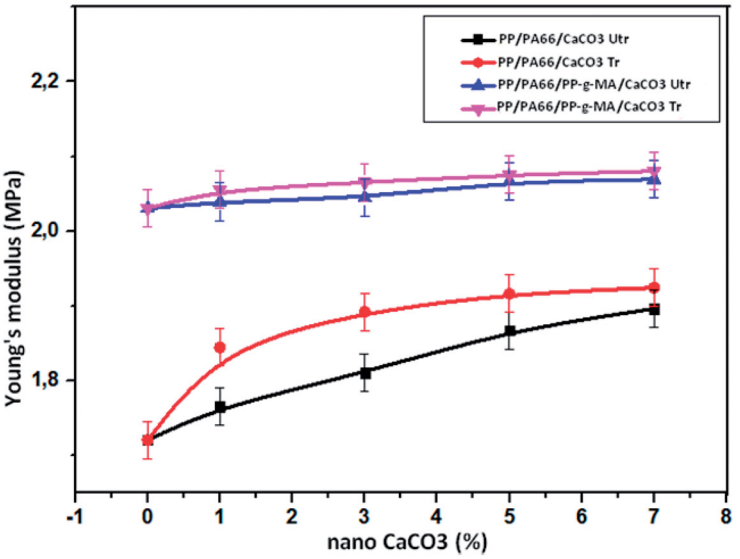

Figure 7. Young's modulus of the different nanocomposites.

Figure 7 shows the variation of Young's modulus of the different materials studied. It is observed that the inclusion of nano-$CaCO_3$ increases the modulus from 1720 to 1959 MPa. The addition of rigid particles to a polymer matrix increases the modulus since the rigidity of inorganic fillers is generally much higher than that of organic polymers. We can also notice an increase in the modulus with increasing content of the inclusion of nano-$CaCO_3$ in (PP/PA66/PP-g-MA), values go from 2030 to 2069 MPa for untreated nano-$CaCO_3$ and to 2073 for treated nanofiller (higher stiffness). This behavior has also been observed with microparticles of $CaCO_3$in PP.[5] The presence of fillers in the matrix hinders the segmental motion of the polymer chains on the application of the tensile stress which can lead to stiffness of the material. Albano[50] in his study on the (PP/$CaCO_3$) composite reported an increase in the modulus and a decrease in the elongation at break indicating a ductile to brittle transition behavior as the $CaCO_3$ content into the blend increases.

Impact tests

The impact resistance of a composite is influenced by many factors including the toughness properties of the reinforcement the nature of the interface region and the matrix. These parameters are extremely important and directly related to the final toughness properties of the obtained composite. Figure 8A shows the impact strength of (PP/PA66) with 1, 3, 5, and 7% by weight of untreated and treated $CaCO_3$.

The introduction of the PP-g-MA in the mixture (PP/PA66/$CaCO_3$) increases the impact strength remarkably from 4.95 to 24.75 KJ/m^2 (Figure 8B). It is believed that this improvement is a manifestation of a better affinity between the compatibilizer and the matrix induced by the

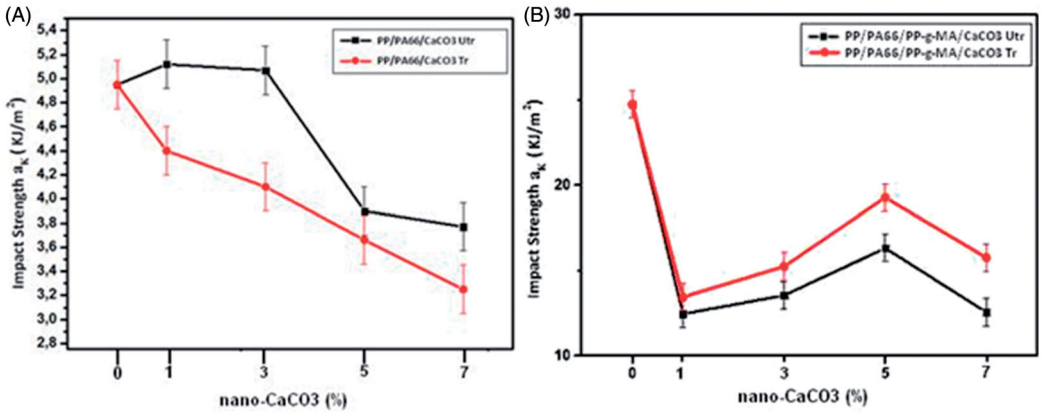

Figure 8. Impact strength of (A) PP/PA66 and (B) PP/PA66/PP-g-MA with 1, 3, 5, and 7% by weight of untreated and treated nano-$CaCO_3$.

formation of a copolymer at the interface able to cushion shocks and leads to a more uniform distribution of impact energy. This result is in agreement with the work of Gharehbash et al.[51] The presence of nano-$CaCO_3$ affects the impact properties of the (PP/PA66) (70/30 wt./wt.) composite, the impact energy values are lower compared to the neat matrix, for a high ratio, there is a decrease in the impact resistance. The increase in $CaCO_3$ content reduces the distance between particles, the impact applied will be absorbed by particular areas of the material generating a localized concentration of forces phenomenon thus leading to a non-homogeneous material from the energy point of view. These results probably reflect, on the one hand, the state of dispersion of the charge within the matrix and, on the other hand, interfacial adhesion, this regression could be due to a phenomenon of compatibility between two completely dissimilar materials. These results are in agreement with morphological observations. The strong embrittlement of nanocomposites made from $CaCO_3$ treated with stearic acid is nevertheless attributed to a strong rigidification of the interfacial zone by the reaction between stearic acid carried on $CaCO_3$ and PA66 matrix. Average values of the impact resistance are obtained with the untreated filler; this result has been confirmed by SEM analysis. These results are comforted by other researchers, Abou El Fettouh et al.[52] Hernandez et al.[19] and Yan et al.[32] reported similar trends in the tensile and impact strength of PP/$CaCO_3$ nanocomposites where they found that the better properties were around 6 to 7 wt.% $CaCO_3$ content while we found that a 5 wt.% $CaCO_3$ gave us the best results. Xia et al.[53] reported in their studies that the addition of 10 wt.% PP-g-MA improves the adhesion between the two polymers and increases the impact resistance of the (PP/PA/MMT) system. Dogu et al.[54] studied the effect of incorporating the compatibilizer EVA-g-MA in the (PP/EVA/nano-tube) mixture, they reported an improvement in impact resistance following a good dispersion of the nano-tube in the blend. Also, the same results were found by Doufnoune et al.[55] in their study on the (LDPE/$CaCO_3$) mixture.

Conclusions

Within the limitations of this study highlights of the major findings are summarized as follows:

According to the Fourier Transform Infrared (FT-IR) spectroscopy and the Scanning Electron Microscopy (SEM) analysis; the addition of PP-g-MA into the (PP/PA66/$CaCO_3$) composite suggests the existence of possible interface interactions on one hand between PP-g-MA and PA66 and, on the other hand, between stearic acid and PA66. The nanosized $CaCO_3$ particles appear to be homogeneously dispersed into the blend and ductile fracture facies of the matrix are observed when a fixed amount of PP-g-MA is incorporated. The resulting blends display a fine-tuned

morphology with improved ductility. However, the blends without compatibilizer show more rigid facies due to the agglomeration of the nanoparticles inducing an increase in the rigidity of the nanocomposites. From the mechanical responses; it is observed that the incorporation of $CaCO_3$ nanoparticles increased the modulus and the tensile strength of the (PP/PA66) blend but decreased its elongation at break. This effect was more pronounced with the insertion of the compatibilizer and for the treated nano-$CaCO_3$ resulting in enhanced interfacial bonding between PA66 and PP. Also, the elongation at break and impact strength was improved by the use of a compatibilizer. TGA analysis established that the thermal stability of the obtained composites was higher than that of (PP/PA66) alone. According to the XRD results, the $CaCO_3$ nanofillers play the role of an effective nucleating agent in the various (PP/PA66) and (PP/PA66/PP-g-MA) composites by modifying the crystal structure causing ultimately to a certain extent an improvement in the thermal stability.

Acknowledgments

The authors would gratefully like to acknowledge the financial support of DGRSDT (la Direction Générale de la Recherche Scientifique et du Développement Technologique, Algérie) for their support in this work.

ORCID

Safieddine Bahlouli http://orcid.org/0000-0002-6294-1880
Azzedine Makhlouf http://orcid.org/0000-0002-3950-4375
Nacerddine Haddaoui http://orcid.org/0000-0002-1515-0867

References

[1] Utracki, L. A., and C. A. Wilkie (Eds.). 2002. *Polymer Blends Handbook*. Norwell, MA: Kluwer Academic Publishers.
[2] Utracki, L. A. 1995. History of commercial polymer alloys and blends (from a perspective of the patent literature). *Polym. Eng. Sci.* 35:2–17.
[3] Ohlsson, B. H., Hassander B. H., and B. Törnell. 1998. Effect of the mixing procedure on the morphology and properties of compatibilized polypropylene/polyamide blends. *Polymer* 39:4715–4721.
[4] Robeson, L. M. 2007. *Polymer Blends: A Comprehensive Review*. Munich, Germany: Hanser Gardner.
[5] Doufnoune, R. N., Haddaoui , and F. Riahi. 2006. Elaboration and characterization of an organic/inorganic hybrid material: effect of the interface on the mechanical en thermal behavior of PP/$CaCO_3$ composites. *Int. J. Polym. Mater.* 55:815–834.
[6] Jaziri, M., N. Barhoumi, V. Massardier, and F. Melis. 2008. Blending PP with PA6 industrial wastes: effect of the composition and the compatibilization. *J. Appl. Polym. Sci.* 107:3451–3458.
[7] Sacchi, A., L. D. Landro, M. Pegoraro, and F. Severini. 2004. Morphology of isotactic polypropylene–polyamide 66 blends and their mechanical properties. *Euro. Polym. J.* 40:1705–1713.
[8] Ide, F., and C. Hasegawa. 1974. Studies on polymer blend of nylon 6 and polypropylene or nylon 6 and polystyrene using the reaction of polymer. *J. Appl. Polym. Sci.* 18:963–974.
[9] Cheng, L. W., Wang , J. Wang, Y. Cao, G. Li, and Y. Shen. 2013. Morphological structure and mechanical properties of in situ microfibrillar composites of modified PA66 with PP. *J. Appl. Polym. Sci.* 127: 4044–4051.
[10] Aljoumaa, K., and Z. Ajji. 2016. Thermal and mechanical properties of irradiated poly(vinyl chloride)/calcium carbonate composite. *J. Rad. Nucl. Chem.* 24:1451–1465.
[11] Nakamura, Y., Y. Fukuoka, and T. Iida. 1998. Tensile test of poly(vinyl chloride) filled with ground calcium carbonate particles. *J. Appl. Polym. Sci.* 70:311–316.
[12] Ghadami, A., and J. Ghadam. 2015. Influence of $CaCO_3$ micro and nano-particles on the structure and properties of nylon-66. *Bulg. Chem. Comm.* 47:19–34.
[13] Gonzalez-Benito, J., J. Martinez-Tarifa, M. E. Sepúlveda-García, R. A. Portillo, and G. Gonzalez-Gaitano. 2013. Composites based on HDPE filled with $BaTiO_3$ submicrometric particles, morphology, structure and dielectric properties. *J. Polym. Test* 32:1342–1349.

[14] Wong, W., G. Ourieva, M. F. Tse, and H. C. Wang. 2003. Filler-filler interaction and filler-polymer interaction in carbon black and silica filled expo polymer. *Macromol. Symp.* 194:175–184.
[15] Ari, G., and I. Aydin. 2010. Rheological and fusion behaviors of PVC micro- and nano-composites evaluated from torque rheometer data. *J. Vinyl Addit. Technol.* 16:223–228.
[16] Shimpi, N., J. Verma, and S. Mishra. 2010. Dispersion of nano $CaCO_3$ on PVC and its influence on mechanical and thermal properties. *J. Compos. Mater.* 44:211–219.
[17] Zoukrami, F., N. Haddaoui, C. Bailly, M. Sclavons, and R. Legras. 2012. Elongational and shear flow behavior of calcium carbonate filled low density polyethylene: effect of filler particle size, content, and surface treatment. *J. Appl. Polym. Sci.* 123:257–266.
[18] Cao, Z., M. Daly, L. Clémence, L. M. Geever, I. Major, C. L. Higginbotham, and D. M. Devine. 2016. Chemical surface modification of calcium carbonate particles with stearic acid using different treating methods. *J. Appl. Surf. Sci.* 378:320–329.
[19] Hernández, Y., T. Lozano, A. B. Morales-Cepeda, F. Navarro-Pardo, M. E. Ángeles, L. Morales-Zamudio, J. A. Melo-Banda, S. Sánchez-Valdes, G. Martínez-Colunga, and F. Rodríguez. 2019. Stearic acid as interface modifier and lubricant agent of the system: polypropylene/calcium carbonate nanoparticles. *Polym. Eng. Sci.* 59:E279–E285.
[20] Chan, C., J. Wu, J. Li, and Y. Cheung. 2002. Polypropylene/calcium carbonate nanocomposites. *Polymer* 43: 2981–2992.
[21] Chongprakobkit, S., M. Opaprakasit, and S. Chuayjuljit. 2007. Use of PP-g-MA prepared by solution process as compatibilizer in polypropylene/polyamide 6 blend. *J. Mater. Mine.* 17:9–16.
[22] Herzberg, G. 1949. Molecular spectra and molecular structure. In *Spectra of Diatomic Molecules*, 2nd ed. New York, NY: D. Van Nostrand Reinhold.
[23] Pai, R., and S. Pillai. 2008. Nanoparticles of amorphous calcium carbonate by mini emulsion: synthesis and mechanism. *J. Cryst.-Eng.-Comm.* 10:865–875.
[24] Bouzidi, F., M. Ghessoum, and N. Haddaoui. 2017. Viscoelastic, thermo-mechanical and environmental properties of composites based on polypropylene/poly(lactic acid) blend and copper modified nanoclay. *J. Adh. Sci. Tech.* 32:596–615.
[25] Miao, M., C. Wei, Y. Wang, and Y. Qian. 2018. Effect of compatibilizer on the interface bonding of graphene oxide/polypropylene composite fibers. *Polymer* 10:1283.
[26] Basilia, M., A. Blessie, G. Marian-Elaine, N. Panganiban, V. Archilles, and D. Michael-Oliver. 2007. Study on the functionality of nano-precipitated calcium carbonate as filler in thermoplastics. *J Solid Mech. Mater. Eng.* 1:564–570.
[27] Seul, S. D., S. R. Lee, and Y. H. Kim. 2004. Poly (methyl methacrylate) encapsulation of calcium carbonate particles. *J. Polym. Sci. A Polym. Chem.* 42:4063–4073.
[28] Arroyo, M., M. A. Lopez-Manchado, and F. Avalos. 1997. Crystallization kinetics of polypropylene: effect of the addition of short glass fibers. *Polymer* 38:5587–5593.
[29] Li, L., C. Y. Li, C. Ni, L. Rong, and B. Hsiao. 2007. Structure and crystallization behavior of nylon 66/multi-walled carbon nanotube nanocomposites at low carbon nanotube contents. *Polymer* 48:3452–3460.
[30] Chatterjee, A., and S. Mishra. 2013. Rheological, thermal and mechanical properties of nano-calcium carbonate ($CaCO_3$)/poly methyl methacrylate (PMMA) core-shell nanoparticles reinforced polypropylene (PP) composites. *Macromol. Res.* 21:474–483.
[31] Khan, I., and A. Bhat. 2014. Micro and nano calcium carbonate filled natural rubber composites and nanocomposites. In *Natural Rubber Materials*, ed. S. Thomas, C. H. Chan, L. Pothen, J. Joy, and H. Maria, pp. 467–487. London, UK: The Royal Society of Chemistry.
[32] Yan, K., W. Guo, H. Mao, Q. Yang, and Z. Meng. 2020. Investigation on foamed PP/Nano-$CaCO_3$ composites in a combined in-Mold decoration and microcellular injection molding process. *Polymer* 12:363–378.
[33] Ulrich, M., C. Caze, and P. Laroche. 1998. Morphological studies of glass-microbead-filled polyamide 6.6-Polypropylene blends. *J. Appl. Polym. Sci.* 67:201–208.
[34] Holsti, R., and J. Seppala. 1992. Effects of compatibilizer on the properties of polyamide/polypropylene blends. *J. Polym. Eng. Sci.* 32:868–877.
[35] Tang, T., A. Lei, and B. Huang. 1996. Studies of morphology and crystallization of PP/PA12 blends. *J. Polym. Sci.* 37:3219–3226.
[36] Zeng, N., S. L. Bai, C. G'Sell, J.-M. Hiver, and Y. W. Mai. 2002. Study on the microstructures and mechanical behavior of compatibilized polypropylene/polyamide 6 blends. *Polym. Int.* 51:1439–1447.
[37] Roeder, J., R. V. B. Oliveira, M. C. Gonçalves, V. Soldi, and A. Pires. 2002. Polypropylene/polyamide-6 blends: influence of compatibilizing agent on interface domains. *J. Polym. Test* 21:815–821.
[38] Zoukrami, F., N. Haddaoui, C. Vanzeveren, M. Sclavons, and J. Devaux. 2008. Effect of compatibilizer on the dispersion of untreated silica in a polypropylene matrix. *Polym. Int.* 57:756–763.

[39] Schlickmann, K., J. Howarth, and D. Kasper Silvia. 2019. Effect of the incorporation of micro and nanoparticles of calcium carbonate in poly (vinyl chloride) matrix for industrial application. *Mater. Res.* 22: 880–892.
[40] Zhang, J. 2006. Influence of compounding route on the properties of polypropylene/nano-$CaCO_3$-ethylene-propylene-dien-polymer component composite. *J. Polym. Sci.* 99:2268–2272.
[41] Bonse, B. C., and L. M. Molina. 2016. Effect of calcium carbonate particle size and content on polyamide 6 processing and properties. *AIP Conf. Proc.* 10:3021.
[42] Sadeghi, M., and A. Esfandiari. 2012. The effects of micro and nano $CaCO_3$ on the rheological and physic/mechanical behavior an SBS/$CaCO_3$ composite. *Mater. Technol.* 6:695–703.
[43] Mao, G., B. He, W. Guo, L. Hua, and Q. Yang. 2018. Effects of Nano-$CaCO_3$ content on the crystallization, mechanical properties, and cell structure of PPNanocomposites in microcellular injection molding. *Polymer* 10:1160.
[44] Nekhamanurak, B., P. Patanathabutr, and N. Hongsriphan. 2014. The influence of micro-/nano-$CaCO_3$ on thermal stability and melt rheology behavior of poly(lactic acid). *EnergProcedia* 56:118–128.
[45] Tang, Y., R. Hu, R. Zhang, Z. Wang, Z. Gui, Z. Chen, and W. Fan. 2004. Investigation into poly(propylene)/clay/calcium carbonate nanocomposites. *Macromol. Mater. Eng.* 289:191–197.
[46] Lam, T. D., T. V. Hoang, D. T. Quang, and J. S. Kim. 2009. Effect of nano sized and surface modified precipitated calcium carbonate on properties of $CaCO_3$/polypropylene nanocomposites. *J. Mater. Sci. Eng.* 501: 87–93.
[47] Kouini, B., and A. Serier. 2012. Properties of polypropylene/polyamide nanocomposites prepared by melt processing with a PP-g-MAH compatibilizer. *J. Mater. & Design.* 34:313–318.
[48] Bordes, M. 2005. Elaboration of composites with $CaCO_3$ precipited. *J. Polym. Eng. Sci.* 41:10–12.
[49] Makhlouf, A., A. Layachi, I. Kouadri, A. Belaadi, and H. Satha. 2020. Structural study and thermal behavior of composites: polyamide 66/glass fibers: the reinforcement ratio effect on the kinetics of crystallization. *J. Compos. Mater.* 54:1467–1481.
[50] Albano, C., J. González, M. Ichazo, C. Rosales, C. Urbina de Navarro, and C. Parra. 2000. Mechanical and morphological behavior of polyolefin blends in the presence of $CaCO_3$. *J. Compos. Struc.* 48:49–58.
[51] Gharehbash, N., and S. Alireza. 2015. Assessment of scattering rate and mechanical properties of blends of polypropylene/polyamide containing modified nano clay and compatibilizer. *Orient J. Chem.* 31:262.
[52] Abou El-Fettoh, A. H., A. El-Sawey, A. M. Motawie, and A. I. Eid. 2018. Study of some polypropylene nanocomposite properties. *Egyp. J. Chem.* 61:825–842.
[53] Xia, M., and Z. Yao. 2014. A potential bio-filler: the substitution effect of furfural modified clam shell for carbonate in polypropylene. *J. Compos. Mater.* 10:6–7.
[54] Dogu, S., E. Tekey, and S. Sen. 2019. Effects of EVA-g-MA and EVACO compatibilizer/toughness on morphological and mechanical properties of PP/EVA/HNT blend polymer nanocomposites. *J. Compos. Mater.* 35:1–15.
[55] Doufnoune, R., N. Haddaoui, and F. Riahi. 2008. Effects of coupling agents on the tensile properties of calcium carbonate filled LDPE compatibilized with maleic anhydride-g-LDPE. *Int. J. Polym. Mater.* 57: 295–318.